Supporting information

Engineered vitamin E-tethered non-immunogenic facial lipopeptide for developing improved siRNA based combination therapy against metastatic breast cancer.

Table of Contents

Figure S16. Cytotoxicity analysis of lipopeptides at 72 h time point in 4T1 murine breast cancer cell line.

Figure S17. Cytotoxicity analysis of lipopeptides at 72 h time point in human fibroblast cell line.

Figure S18. Cytotoxicity analysis of lipopeptides at 72 h time point in human embryonic kidney cell line HEK-293.

Figure S19. Cytotoxicity analysis of lipopeptides_Notch1 complex (MR 50:1) at 48 h time point in MDA-MB-231 breast cancer cell line.

Figure S20. Chemical structure of lipopeptides used for computational studies with the substituents (a) adamantane and (b) Sub-vitE.

Figure S21. Flowcytometry analysis of lipopeptide_siRNA complexes at MR50 in presence of endocytosis inhibitors and actin polymerization inhibitor in MDA-MB-231 cells.

Figure S22. GUV poration assay of early endosome.

Figure S23. Real-Time PCR analysis of percentage of Erk1 gene knockdown at mRNA level in MDA-MB-231 cells by lipopeptide_ERK1/2 silencing siRNA complex after 48 h incubation at molar ratio 50 (lipopeptide:siRNA).

Figure S24. Real-Time PCR analysis of percentage of Erk1 gene knockdown at mRNA level in MDA-MB-231 cells by lipopeptide_ERK1/2 silencing siRNA complex after 72 h of incubation at molar ratio 50 (lipopeptide:siRNA).

Figure S25. Real-Time PCR analysis of percentage of Erk2 gene knockdown at mRNA level in MDA-MB-231 cells by lipopeptide_ERK1/2 silencing siRNA complex after 72 h of incubation at molar ratio 50 (lipopeptide:siRNA).

Figure S26. Immunofluorescence of ERK1/2 protein in MDA-MB-231 cells after transfection with unlabelled lipopeptide AB36_ERK1/2 silencing siRNA complex (MR=50) after 72 h of incubation.

Figure S27. Immunofluorescence of ERK1/2 protein in MDA-MB-231 cells after transfection with HiPerFect_ERK1/2 silencing siRNA complex after 72 h of incubation.

Figure S28. Convergence of free energy surface a) ADM b) sub-vitE.

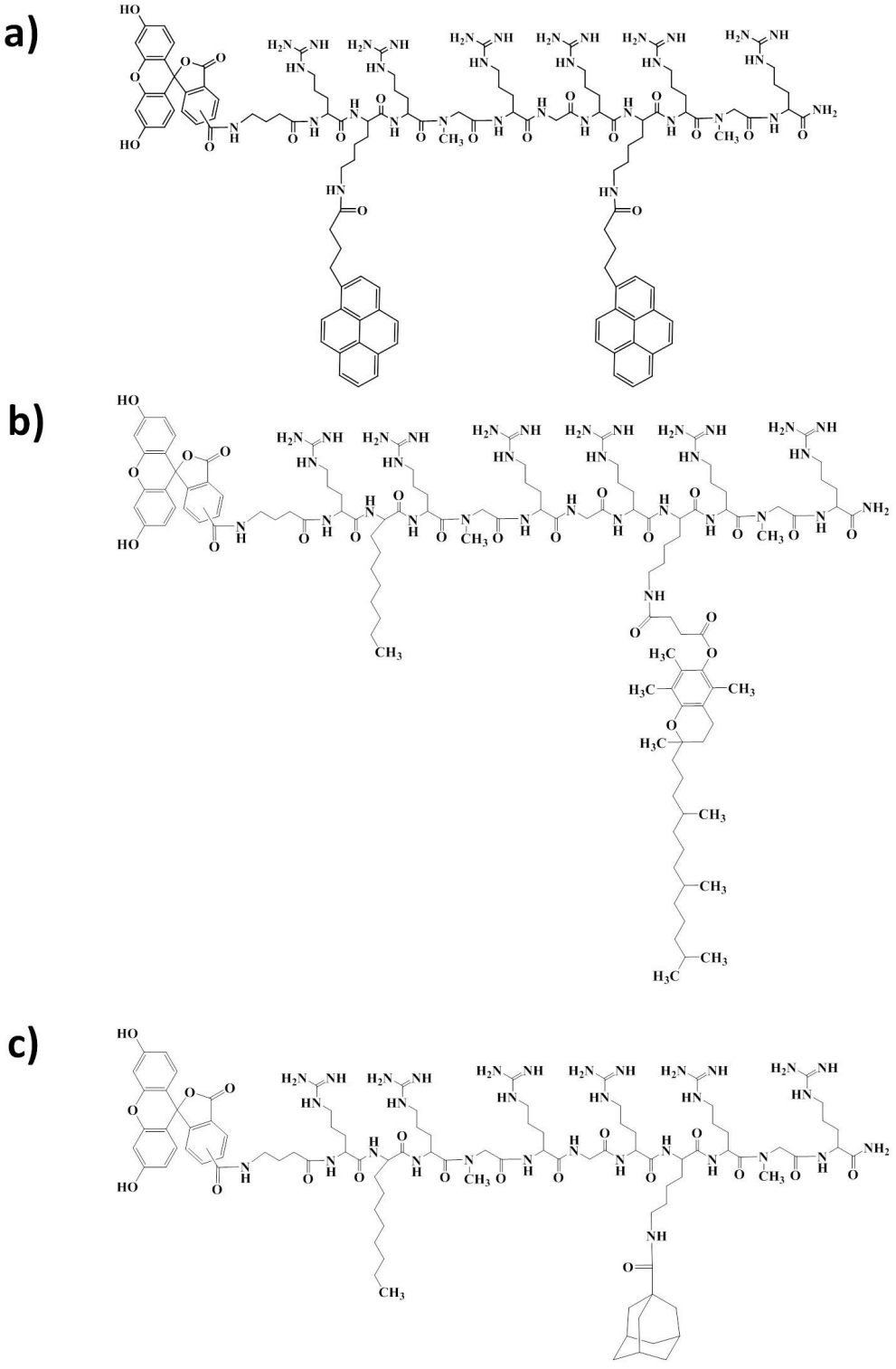

Figure S1. Schematic diagram of lipopeptides a) AB17 b) AB18 c) AB29 using ChemDraw 12.0 software.

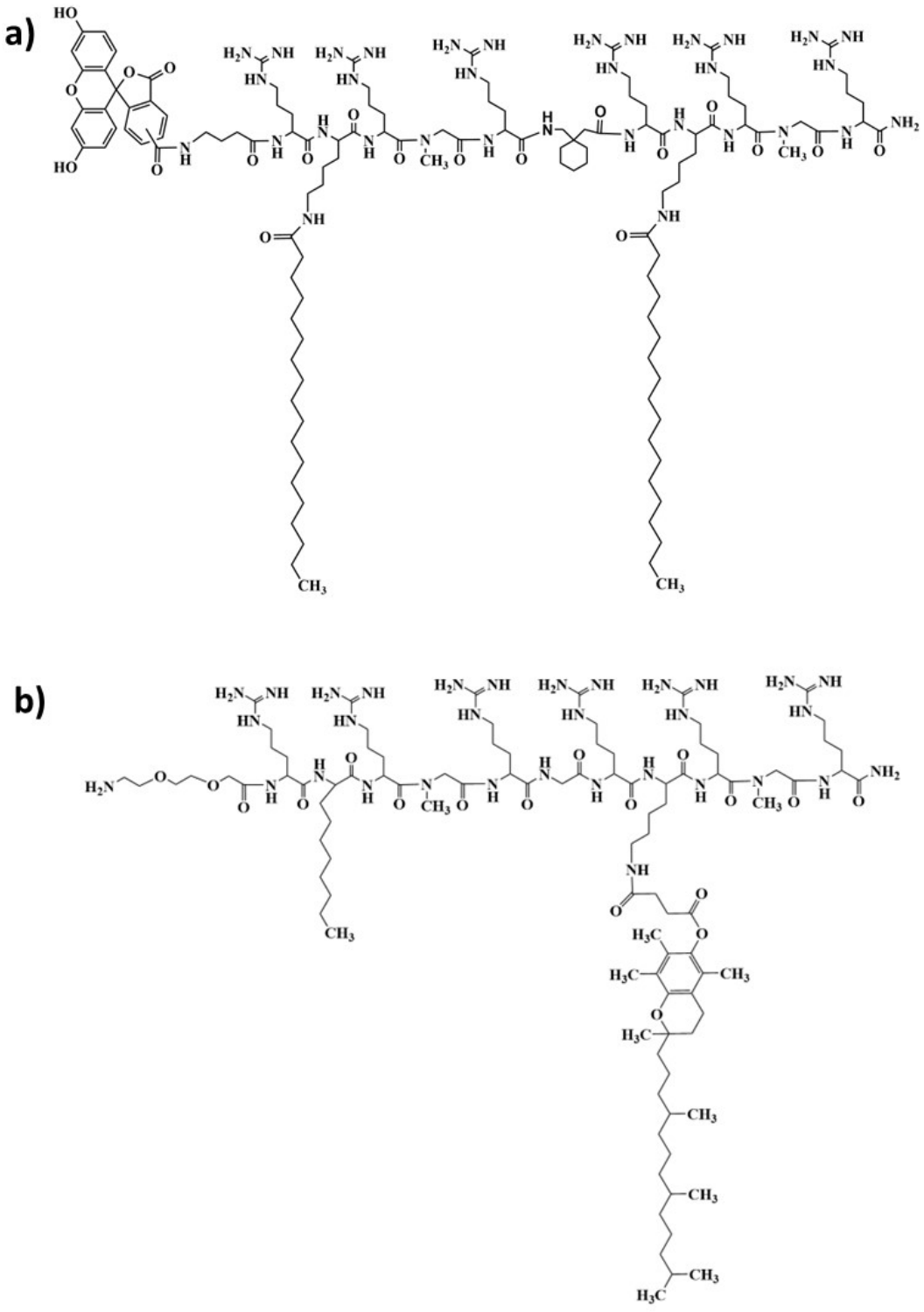

Figure S2. Schematic diagram of lipopeptides a) AB32 b) AB36 using ChemDraw 12.0 software. Please note that the lipopeptide AB18 and lipopeptide AB36 have similar sequences. Lipopeptide AB18 has fluorophore FAM, which is not present in lipopeptide AB36. In lipopeptide AB18, gamma-aminobutyryl residue is present as spacer between peptide chain and fluorophore (FAM). To avoid interference of FAM in certain microscopic studies lipopeptide AB36 is used instead of lipopeptide AB18.

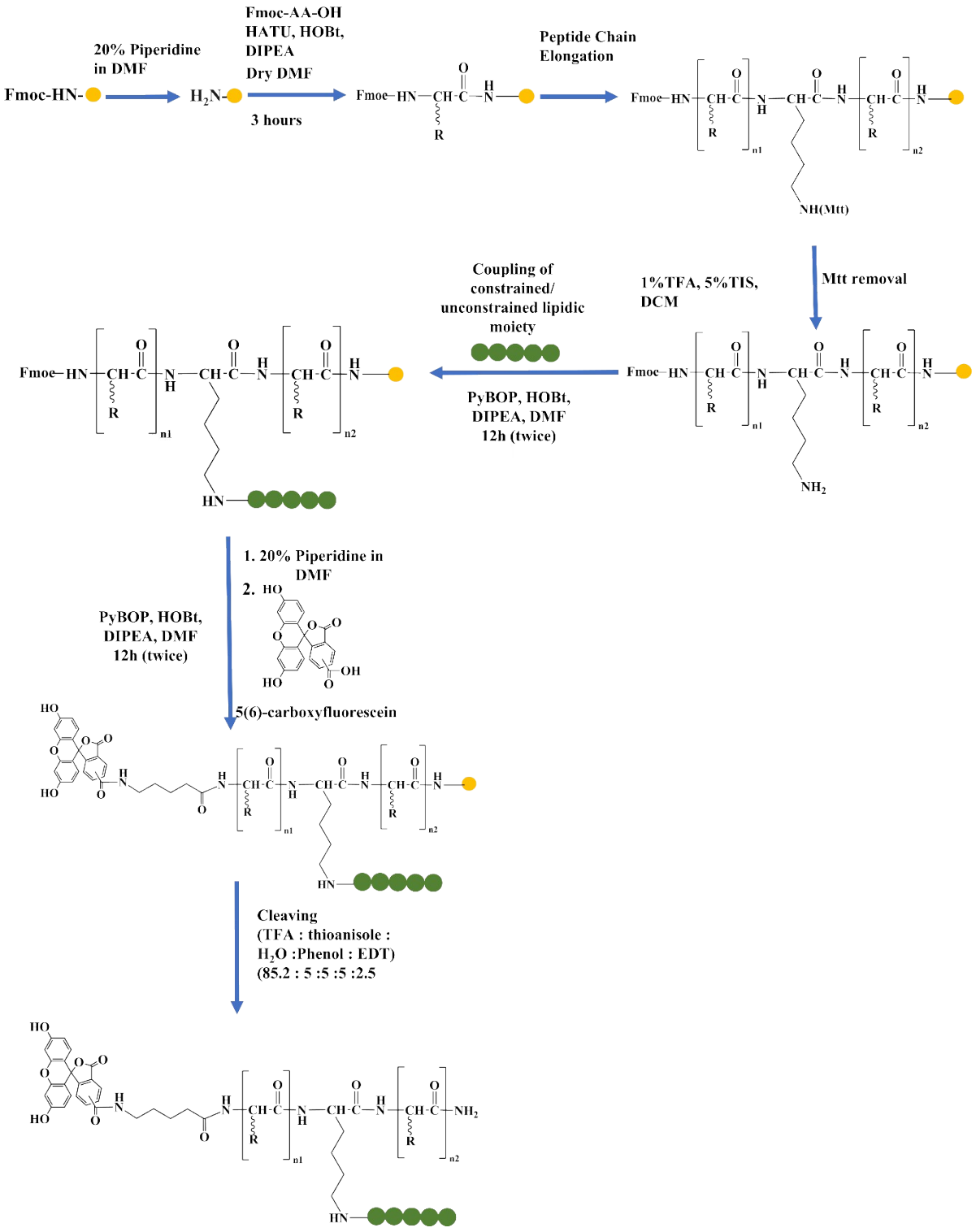

Figure S3. General synthesis scheme of FAM-labelled lipopeptides having constrained or unconstrained lipidic moieties.

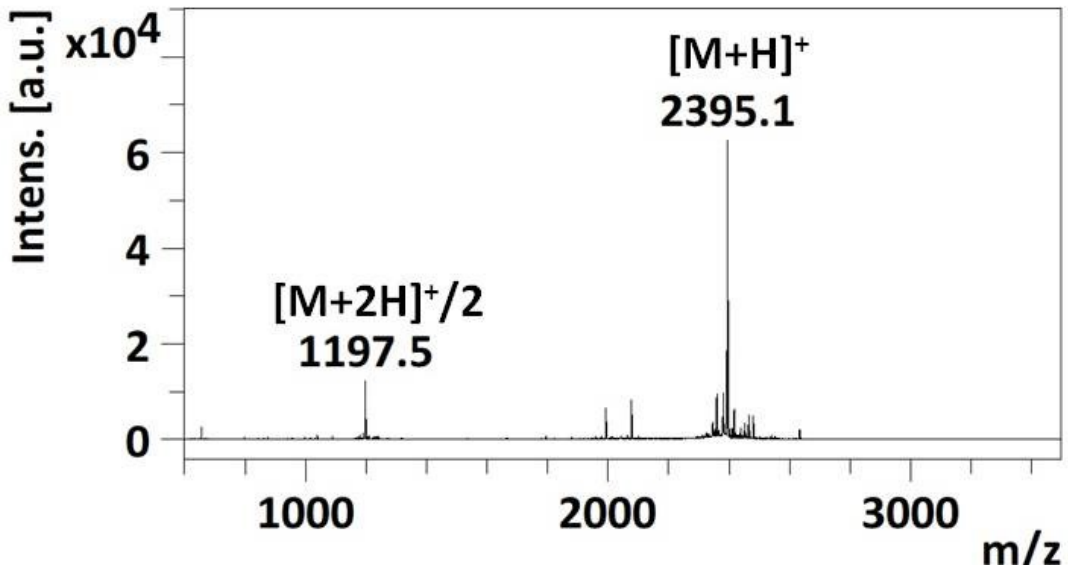

Figure S4. MALDI-TOF mass spectrum of the lipopeptide AB17. Calculated mass: 2394 Da; Observed mass: 2395.1 Da ($[M+H]^+$) and 1197.5 Da ($[M+2H]^+/2$).

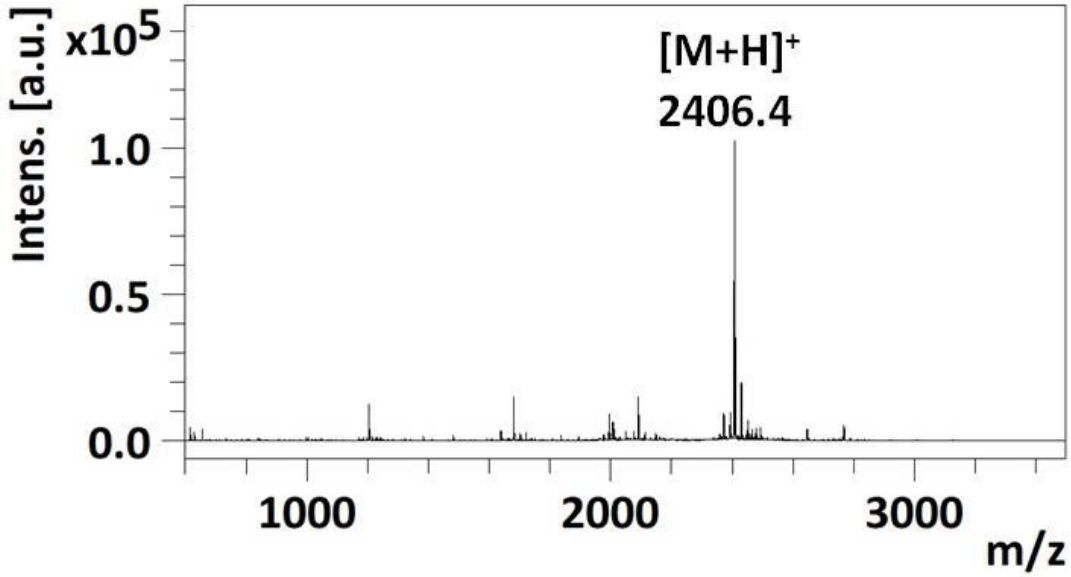

Figure S5. MALDI-TOF mass spectrum of the lipopeptide AB18. Calculated mass: 2405.55 Da; Observed mass: 2406.4 Da ($[M+H]^+$).

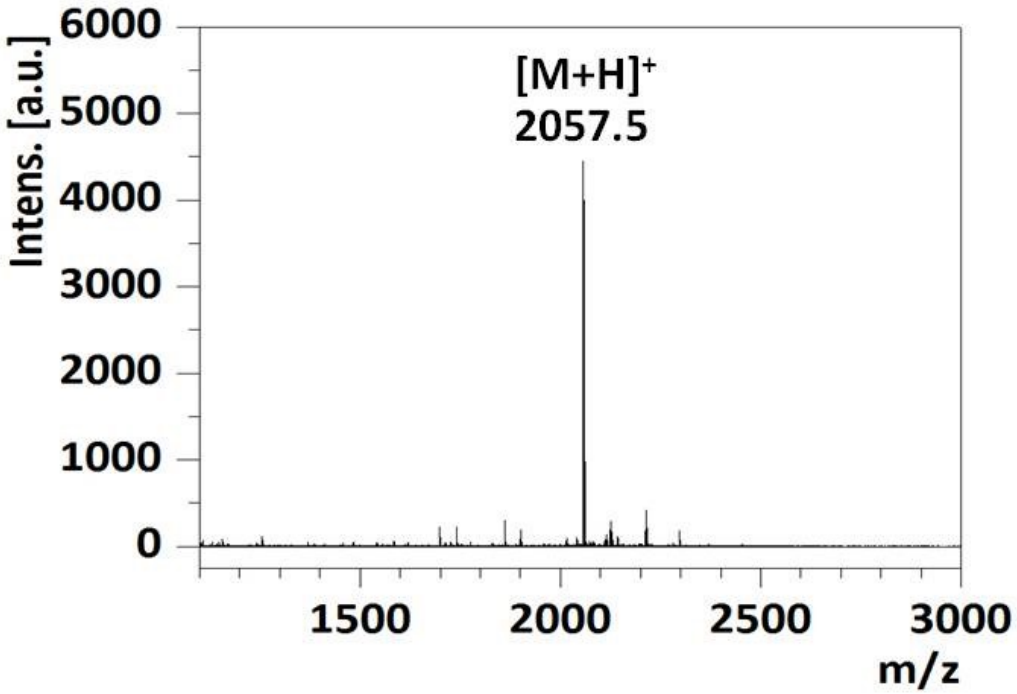

Figure S6. MALDI-TOF mass spectrum of the lipopeptide AB29. Calculated mass: 2056 Da; Observed mass: 2057.5 Da ($[M+H]^+$).

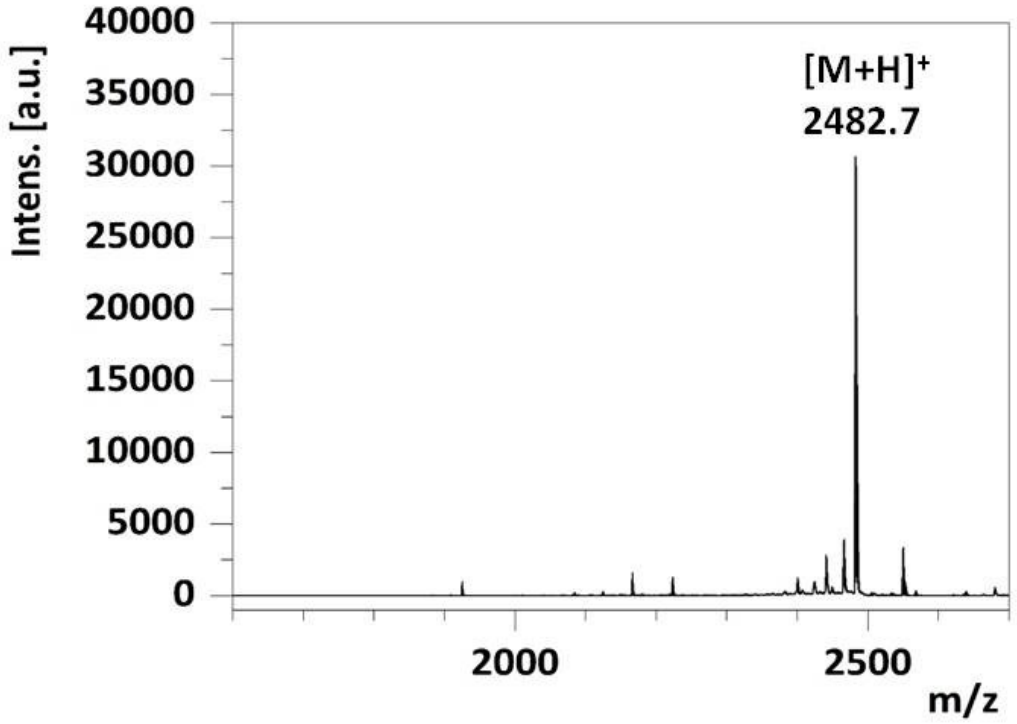

Figure S7. MALDI-TOF mass spectrum of the lipopeptide AB32. Calculated mass: 2481.8 Da; Observed mass: 2482.7 Da ($[M+H]^+$).

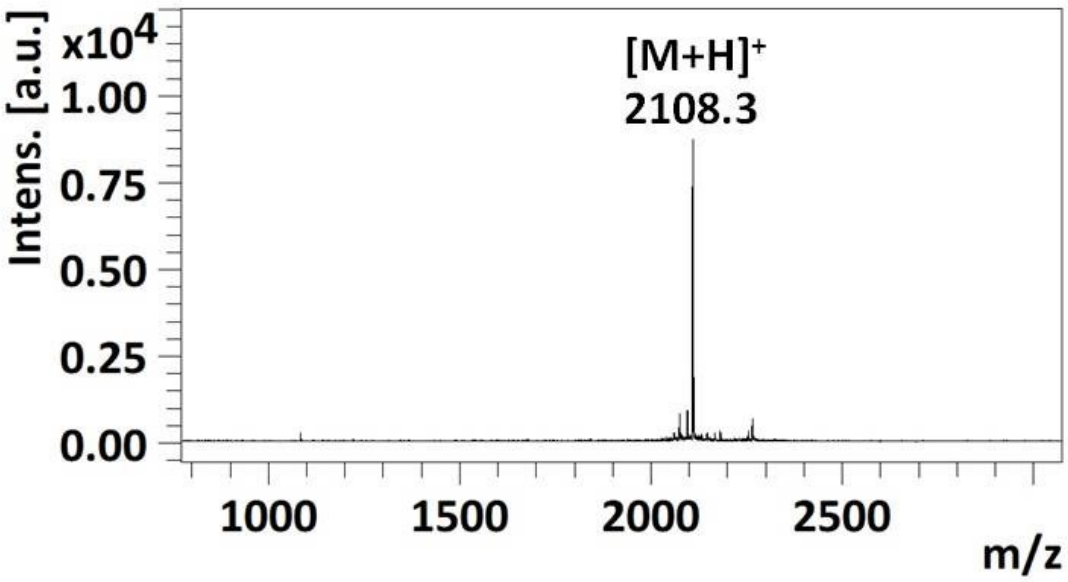

Figure S8. MALDI-TOF mass spectrum of the lipopeptide AB36. Calculated mass: 2107 Da; Observed mass: 2108.3 Da ($[M+H]^+$).

Table S1. Lipopeptide sequences and their mass values observed from MALDI-TOF.

Reference Name	**Sequence**	**Calculated Mass (Da)**	**Observed Mass (Da)**
AB17	FAM-γAbu-Arg- Lys-N^{ε}(1-Pyrenebutyryl)-Arg-Sar-Arg-Gly-Arg- Lys-N^{ε}(1-Pyrenebutyryl)-Arg-Sar-Arg-NH_2	2394	2395.1 ($[M+H]^+$) and 1197.5 ($[M+2H]^+/2$)
AB18	FAM-γAbu-Arg- C^{α}-Octylgly -Arg-Sar-Arg-Gly-Arg- Lys-N^{ε}(D-alpha-Tocopherol succinyl)-Arg-Sar-Arg-NH_2	2405.55	2406.4 ($[M+H]^+$)
AB29	FAM-γAbu-Arg-C^{α}-Octylgly-Arg-Sar-Arg-Gly-Arg-Lys-N^{ε}(1-Adamantyl)-Arg-Sar-Arg-NH_2	2056	2057.5 ($[M+H]^+$).
AB32	FAM-$^{\gamma}$Abu-Arg- Lys-N^{ε}(stearyl)-Arg-Sar-Arg-Gpn-Arg- Lys-N^{ε}(stearyl)-Arg-Sar-Arg-NH_2	2481.8	2482.7 ($[M+H]^+$).
AB36	PEG9-Arg- C^{α}-Octylgly -Arg-Sar-Arg-Gly-Arg-Lys-N^{ε}(D-alpha-Tocopherol succinyl)-Arg-Sar-Arg-NH_2	2107	2108.3 ($[M+H]^+$).

FAM is 5(6) carboxyfluorescein dye. PEG residue and gabapentin residue used in this study are designated as PEG9 and Gpn respectively. 8-amino-3,6-dioxaoctanoyl is abbreviated as PEG9.

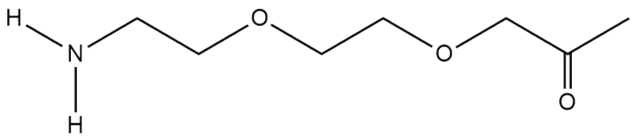

8-amino-3,6-dioxaoctanoyl

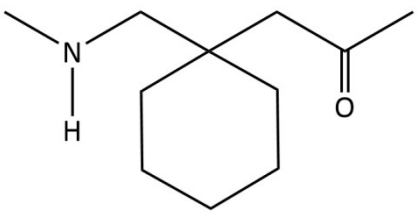

Gabapentin

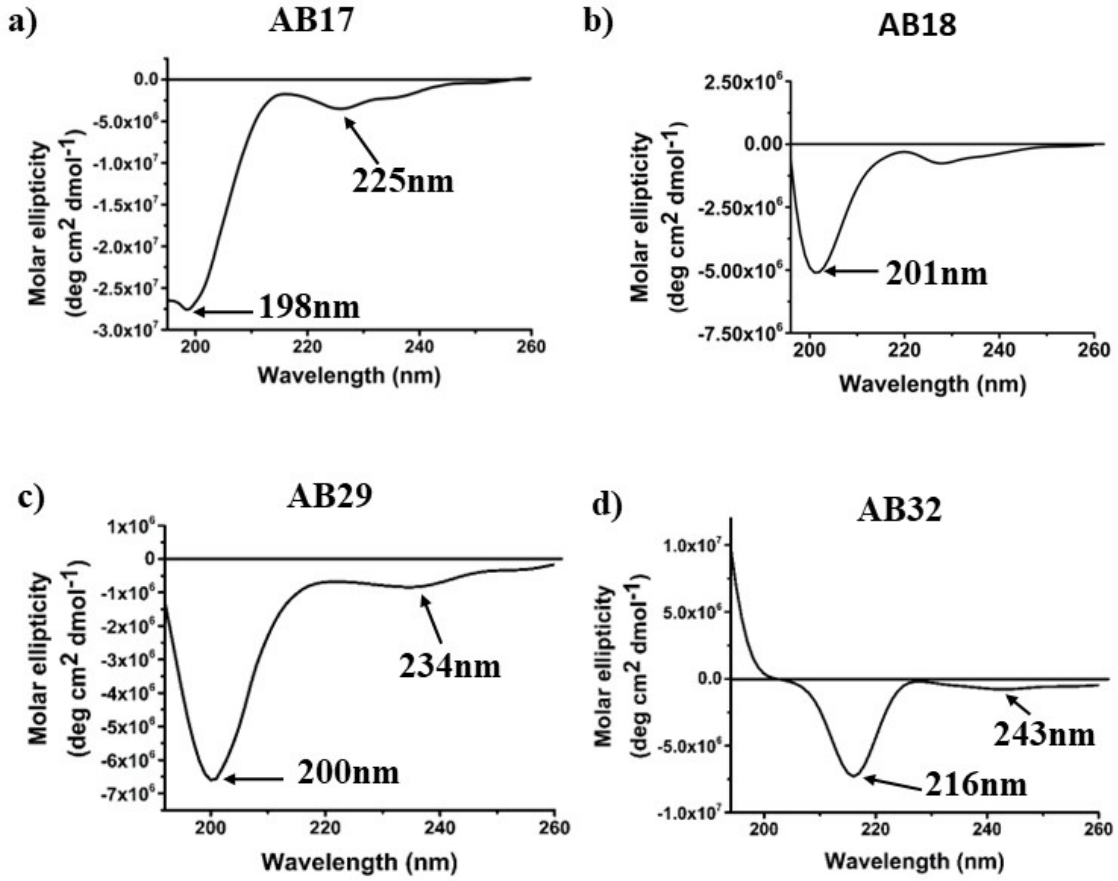

Figure S9. Circular dichroism (CD) spectra of synthesized lipopeptides a) AB17 b) AB18 c) AB29 and d) AB32. All the lipopeptides showed unstructured conformation.

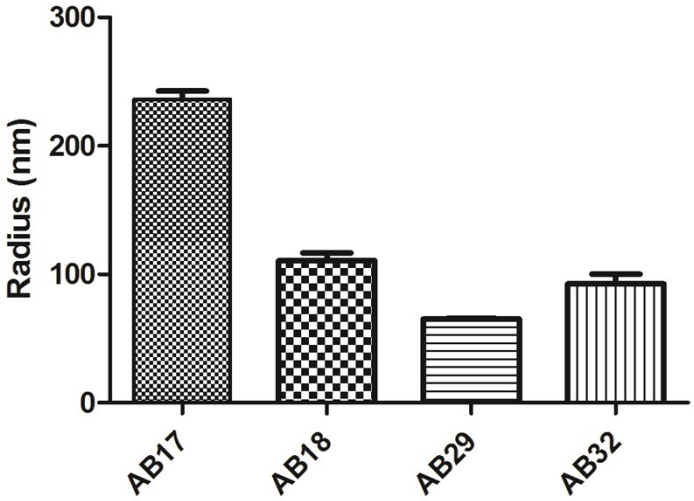

Figure S10. The hydrodynamic radius of lipopeptides AB17, AB18, AB29 and AB32 were found to be 236.12±11 nm, 110.6±10 nm, 65±0.8 nm, and 92.7±12.7 nm, respectively in cell culture media (DMEM+10%FBS). Cell culture media with FBS was used to mimic physiological condition and hydrodynamic radius were measured considering protein corona effect.

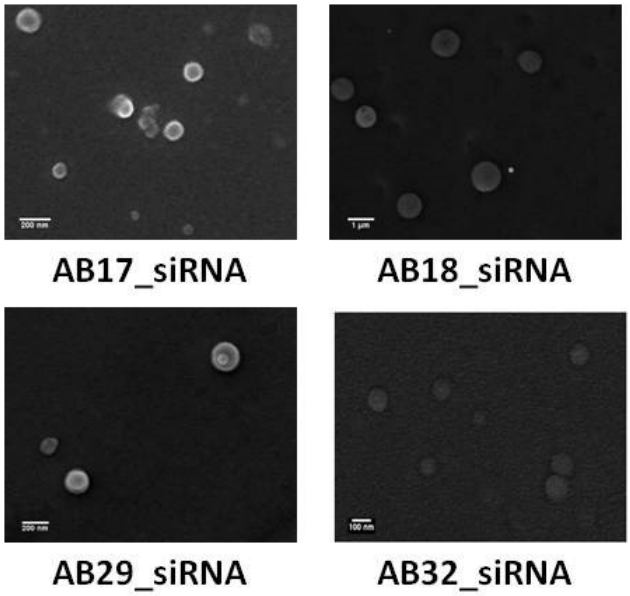

Figure S11. FE-SEM images showing spherical nanostructure of self-assembled lipopeptide_siRNA complexes (MR 50). The average diameter of the self-assembled complexes of lipopeptides AB17, AB29 and AB32 complexed siRNA were 133±22, 182±20, 144±23, and 100±13.6 nm, respectively.

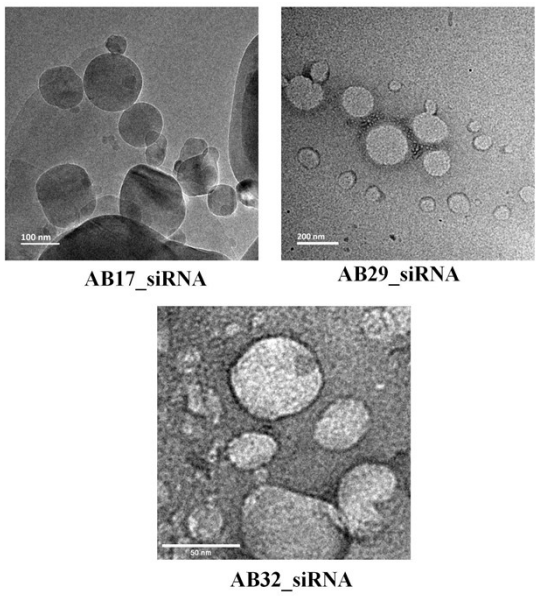

Figure S12. Cryo-TEM images of lipopeptide_siRNA complexes showing spherical nanostructure of self-assembled peptides (MR 50). The average diameter of the self-assembled lipopeptide_siRNA complexes comprising lipopeptides of AB17, AB29 and AB32 are 131.6±24 nm, 99±20 nm, and 59±7.5 nm, respectively.

Table S2: Hydrodynamic radius of lipopeptide_siRNA complexes at different molar ratios (MRs) in cell culture media (DMEM+10%FBS).

Lipopeptides	**Molar ratio (Lipopeptide:siRNA)**				
Lipopeptide code	**5:1 (Radius (nm))**	**10:1 (Radius (nm))**	**20:1 (Radius (nm))**	**50:1 (Radius (nm))**	**100:1 (Radius(nm))**
AB17_siRNA	81±1	55.5±5	105±9.4	114±7	197±2.3
AB18_siRNA	69±15.6	80±14.7	66±2	120±8	116±2.9
AB29_siRNA	58±4	51.5±4	78.6±17.5	66±5.5	97±21
AB32_siRNA	113.6±9.5	98±8	107±14.5	139±9.4	200±10.5

Table S3. Zeta potential value of lipopeptide_siRNA complexes at different molar ratios (MR) from 5 to 100 (MR=lipopeptide:siRNA) of AB17_siRNA, AB18_siRNA and AB36_siRNA complexes.

Molar ratio (MR)	**AB17_siRNA complex**		**AB18_siRNA complex**		**AB36_siRNA complex**	
	Zeta potential (mV)	**Mean Zeta potential (mV)**	**Zeta potential (mV)**	**Mean Zeta potential (mV)**	**Zeta potential (mV)**	**Mean Zeta potential (mV)**
MR5	-8.36	-8.93±1.75	-27.8	-26.0±1.67	-2.76	-2.88±0.13
	-10.9		-25.7		-2.87	
	-7.54		-24.5		-3.03	
MR10	-9.83	-13.48±3.21	-26.2	-25.3±0.78	-0.788	-0.35±0.4
	-15.9		-24.8		-0.247	
	-14.7		-24.9		-0.002	
MR20	-12.8	-14.63±2.02	-27.3	-26.17±1.15	-0.550	-1.20±0.83
	-16.8		-25.0		-0.918	
	-14.3		-26.2		-2.14	
MR50	11.3	12.47±1.77	9.55	10.1±0.71	2.12	2.15±0.56
	14.5		9.84		2.72	
	11.6		10.9		1.60	
MR100	26.6	28.87±4.10	37.1	36.97±0.23	0.433	0.52±0.07
	33.6		36.7		0.581	
	26.4		37.1		0.541	

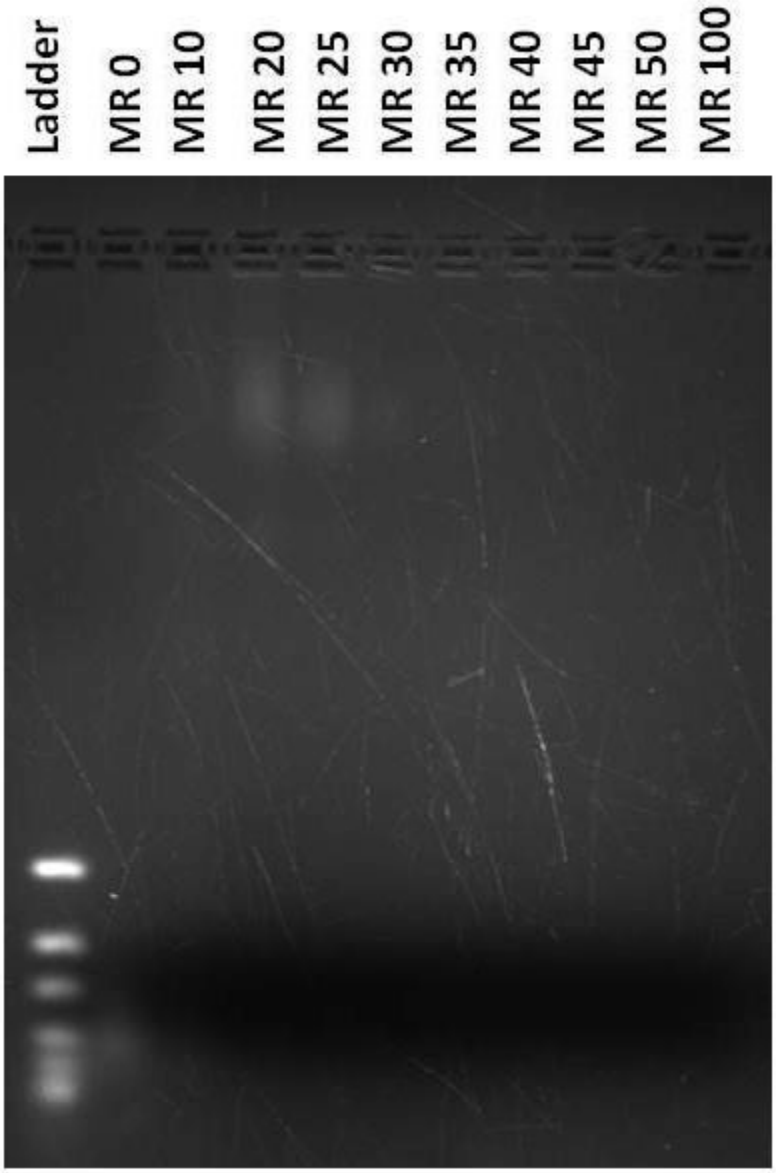

Figure S13. Agarose gel retardation assay of lipopeptide AB18_siRNA complexes at different molar ratios. The lipopeptide AB18 shows complete masking of siRNA at molar ratio 35 and above. Based on this information, in all cell based assay lipopeptide_siRNA MR 50 was used, so the nanocomplex should be positively charged.

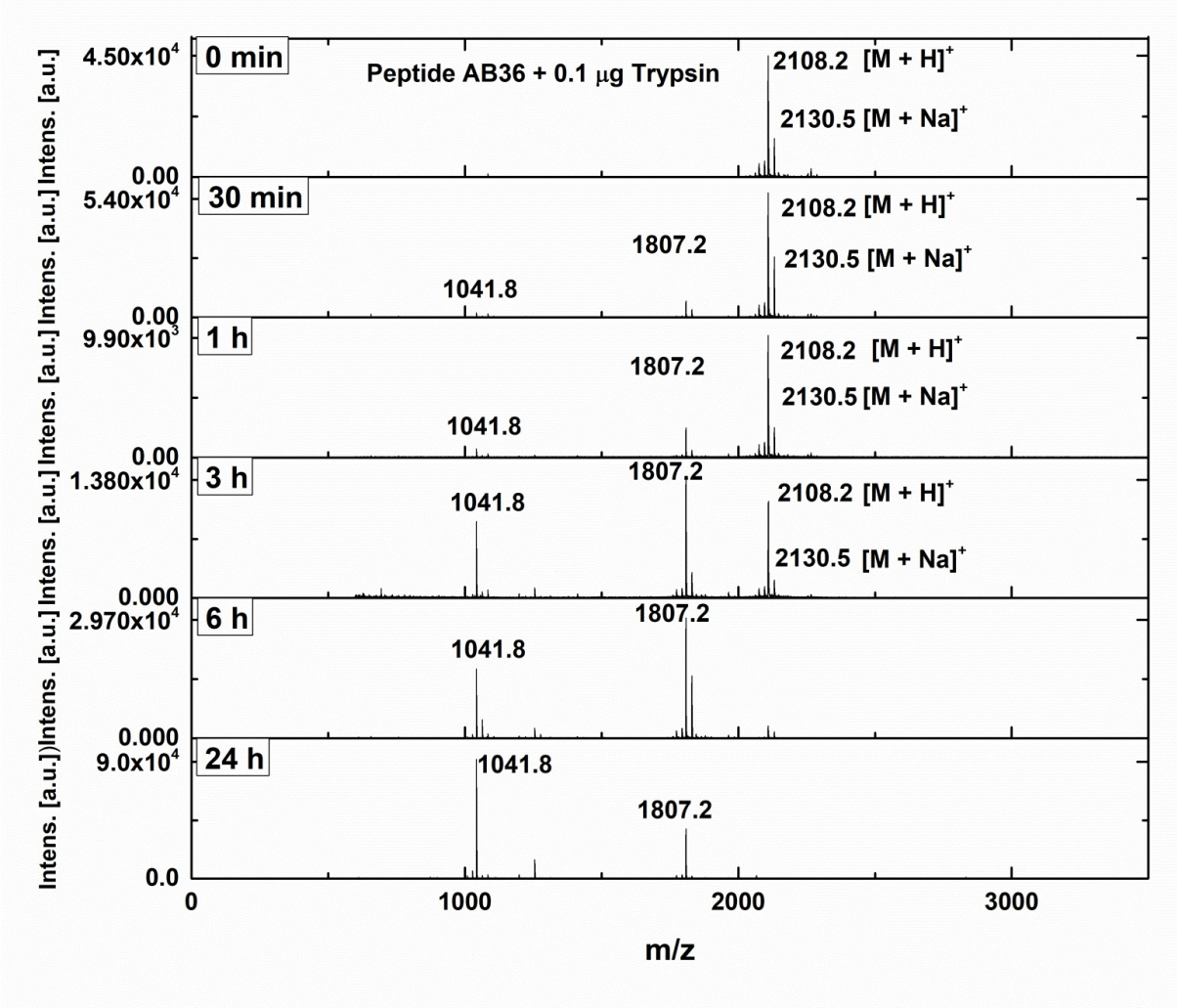

Figure S14. Protease stability assay of lipopeptide AB36. Lipopeptide AB36 showed complete degradation at 6h time point in presence of 0.1 μg trypsin ensuring that these lipopeptides will not be accumulated inside a living system.

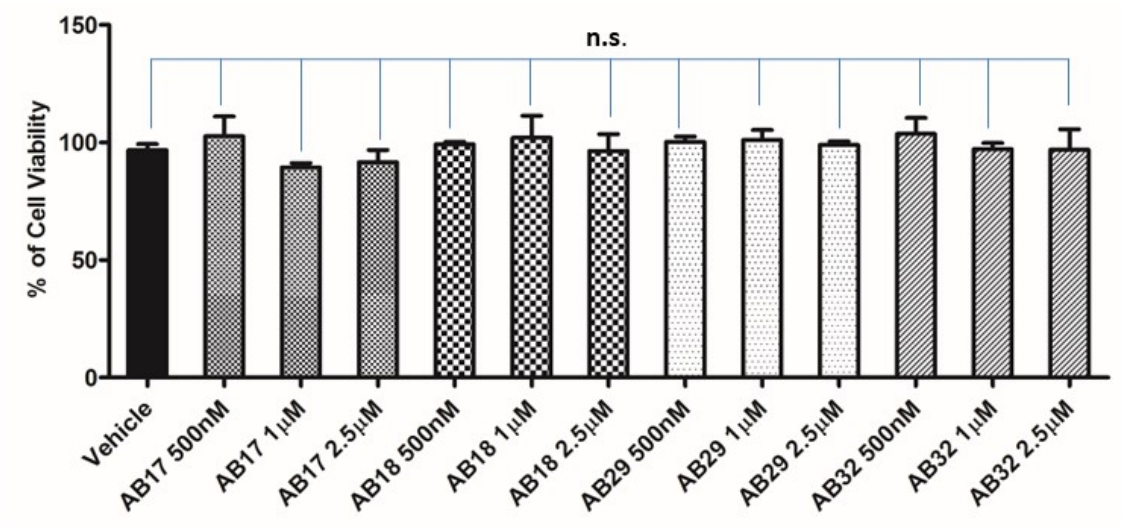

Figure S15. Cytotoxicity analysis of lipopeptides at 72 h time point in MDA-MB-231 breast cancer cell line. Error bars indicate SEM from three separate replicates. The results indicate the lipopeptides synthesized are non-toxic to MDA-MB-231 cells up to 2.5 μM lipopeptide concentration till 72 h time point.

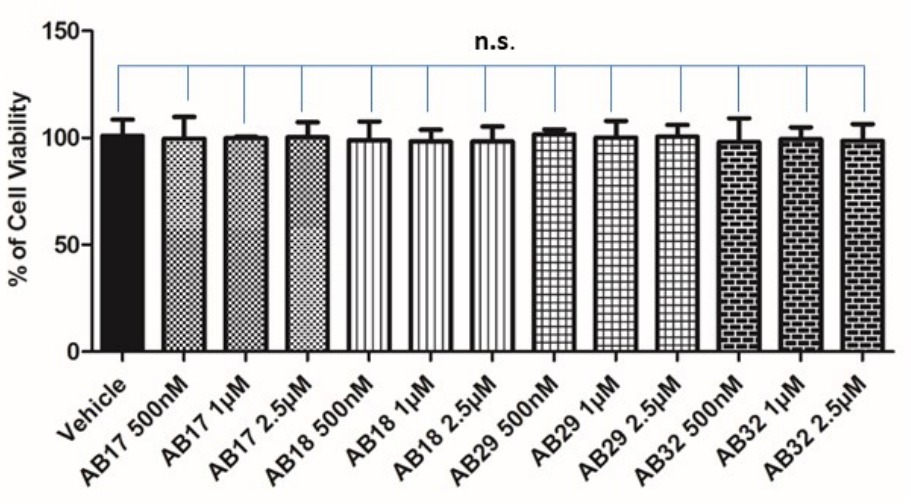

Figure S16. Cytotoxicity analysis of lipopeptides at 72 h time point in 4T1 murine breast cancer cell line. Error bars indicate SEM from three separate replicates. The results indicate the lipopeptides synthesized are non-toxic to 4T1 cells up to 2.5μM lipopeptide concentration till 72 h time point.

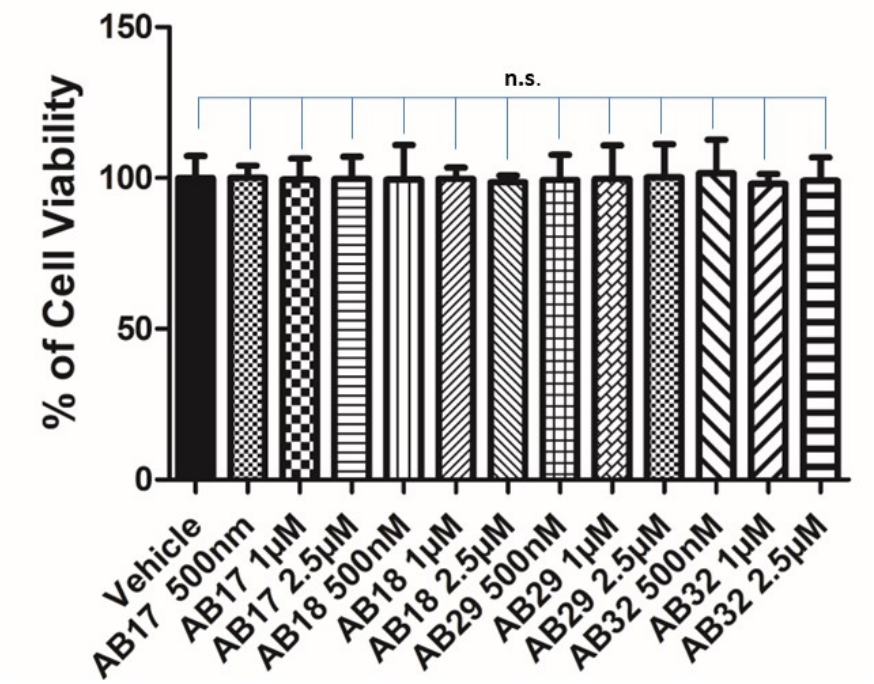

Figure S17. Cytotoxicity analysis of lipopeptides at 72 h time point in non-cancerous human fibroblast cell line. Error bars indicate SEM from three separate replicates. The results indicate the lipopeptides synthesized are non-toxic to human fibroblast cell line up to 2.5µM lipopeptide concentration till 72 h time point.

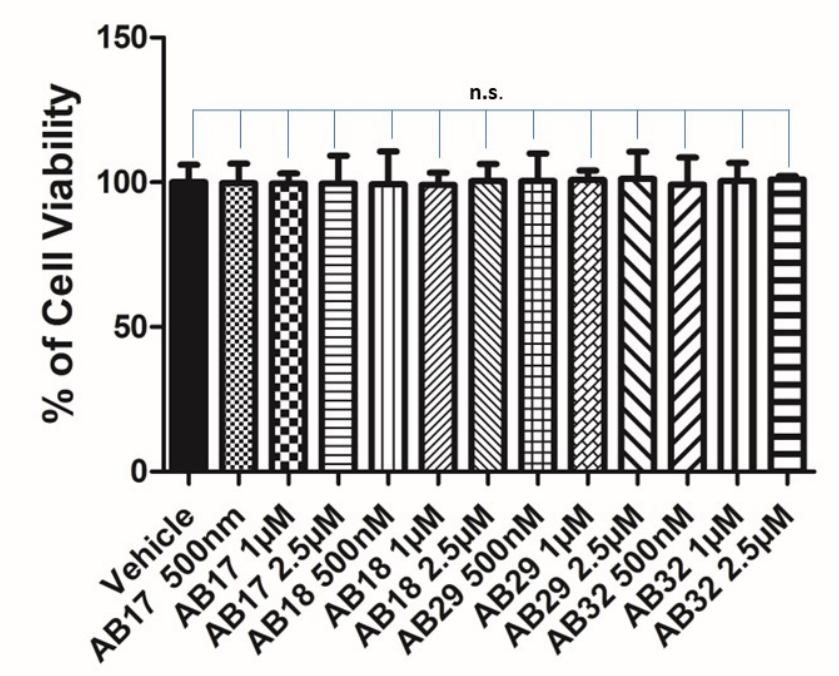

Figure S18. Cytotoxicity analysis of lipopeptides at 72 h time point in non-cancerous human embryonic kidney cell line HEK-293. Error bars indicate SEM from three separate replicates. The results indicate the lipopeptides synthesized are non-toxic to human embryonic kidney cell line HEK-293 up to 2.5µM lipopeptide concentration till 72 h time point.

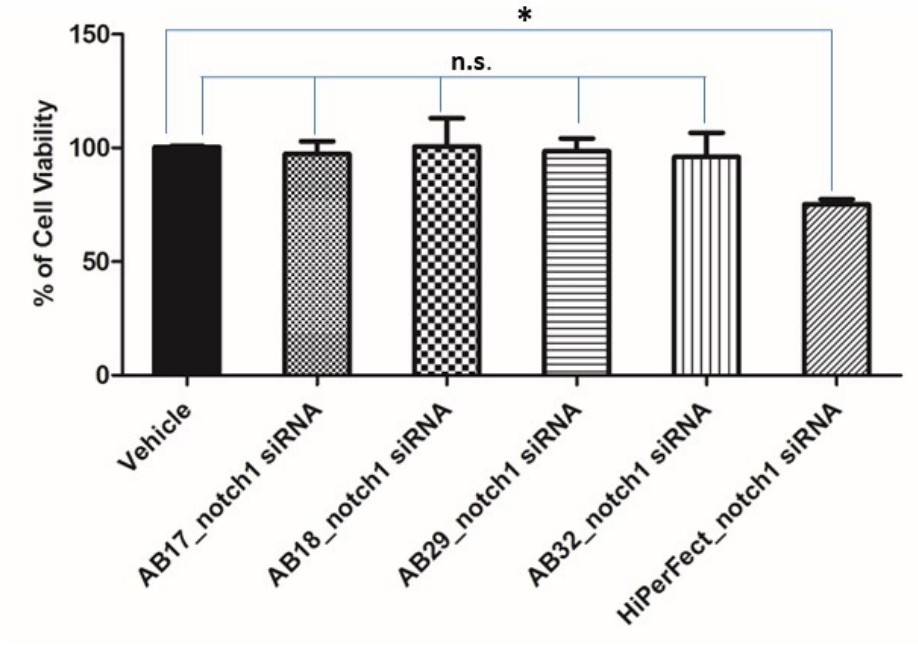

Figure S19. Cytotoxicity analysis of lipopeptides_Notch1 complex (MR 50:1) at 48 h time point in MDA-MB-231 breast cancer cell line. Error bars indicate SEM from three separate replicates. The results indicate the lipopeptides_Notch1 complex (MR 50:1) are non-toxic to MDA-MB-231 cells at 1.25 μM lipopeptide concentration at 48 h time point. HiPerFect_Notch1 complex shows toxicity compared to the synthesized lipopeptide_Notch1 complex at 48 h time point.

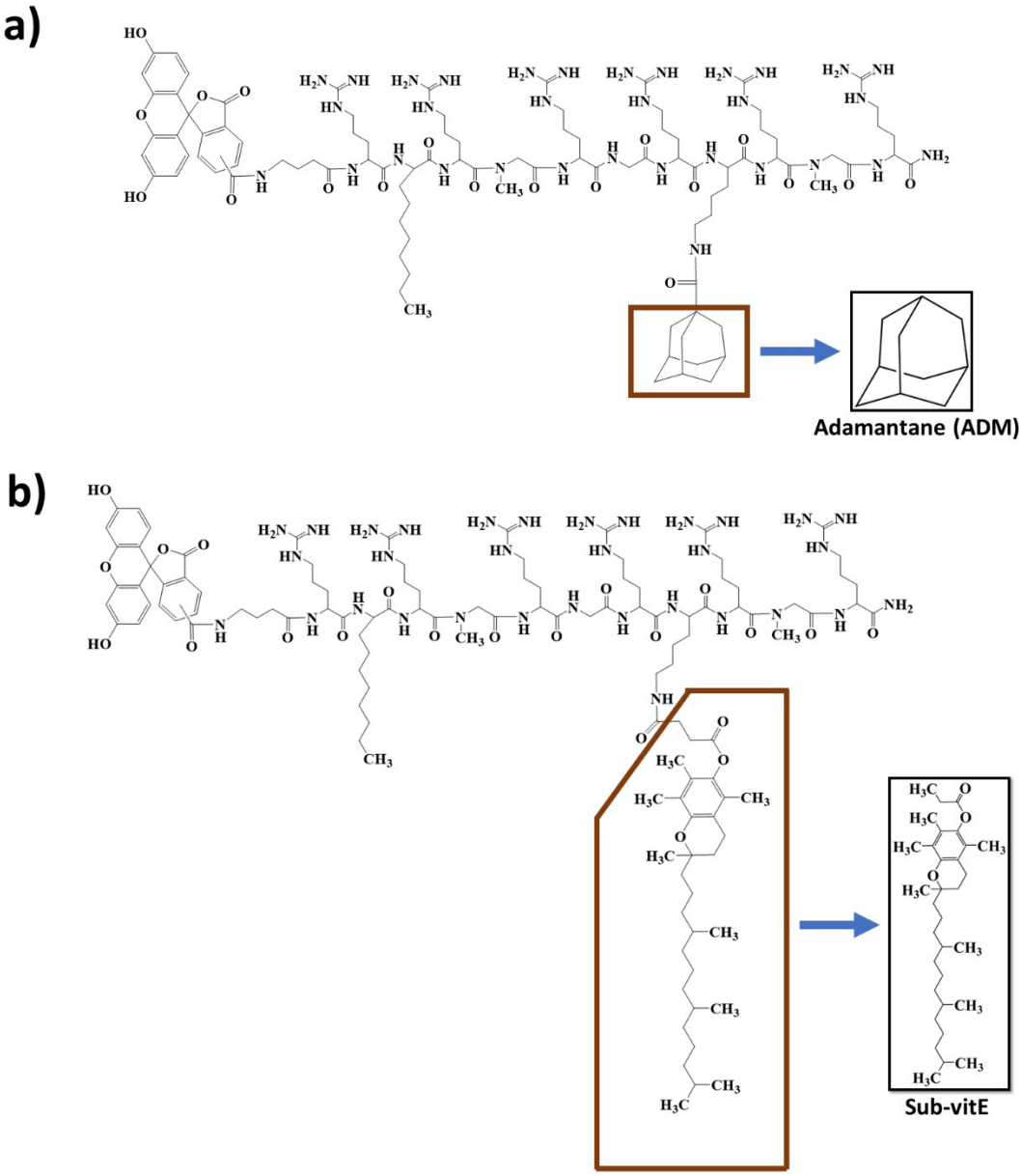

Figure S20. Chemical structure of lipopeptides used for computational studies with the substituents (a) adamantane (ADM) and (b) substituted vitamin-E (Sub-vitE) highlighted in the box. Kindly note that computational studies were performed only for ADM and Sub-vitE.

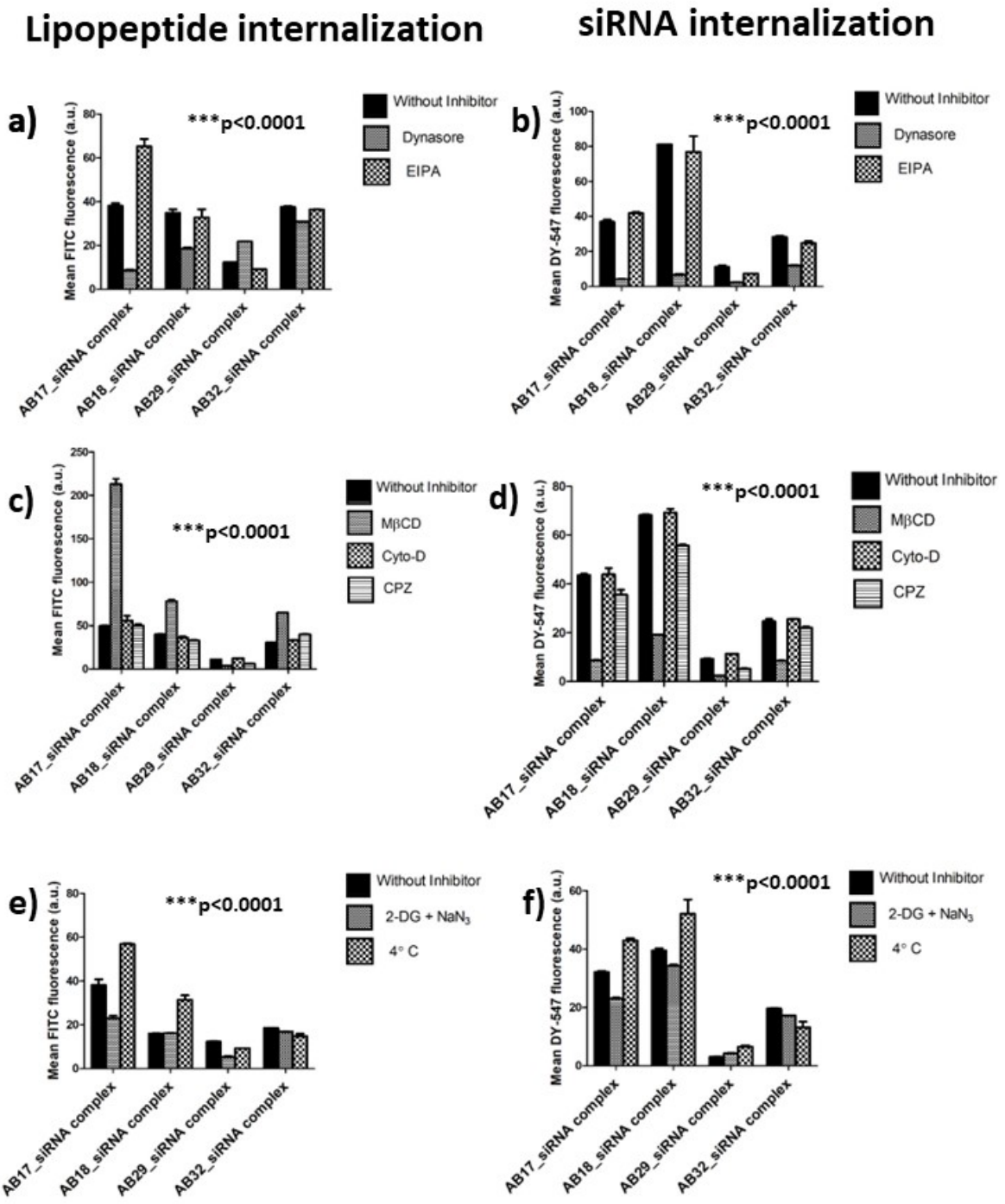

Figure S21. (a-f) Depicts flowcytometry analysis of lipopeptide_siRNA complexes at MR50 in presence of endocytosis inhibitors and actin polymerization inhibitor in MDA-MB-231 cells. Inhibitor of endocytosis, chlorpromazine (30 μM), 5-(N-ethyl-N-isopropyl) amiloride (50 μM), methyl-β-cyclodextrin (3.5 mM) and actin polymerization inhibitor cytochalasin-D (5 μM) are represented as CPZ, EIPA, MβCD and Cyto D, respectively. It was observed that the siRNA internalization shows marked decrease in the presence of 80 μM Dynasore and 3.5 mM of methyl-β-cyclodextrin suggesting the lipopeptide_siRNA complexes are most likely internalized by both clathrin and caveolae dependent endocytosis.

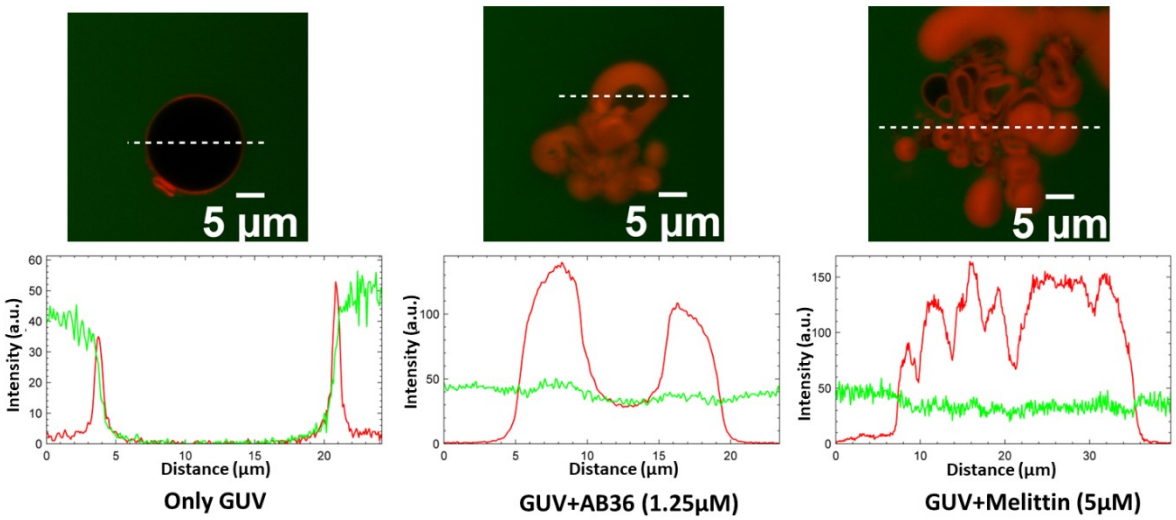

Figure S22. GUV poration assay of early endosome. GUV was prepared mimicking early endosome (PC:PE:cholesterol 65:15:20) by gel assisted method. Melittin, a 26-residue amphipathic membrane active peptide was taken as a positive control. GUV was labelled with CM-Dil and viewed in rhodamine channel. The background of the GUV has buffer containing FAM which is viewed in FITC channel. The untreated GUV (extreme left) is intact and there is no leakage and the FAM containing buffer was not been able to penetrate the GUV. Lipopeptide AB36_siRNA complex and melittin upon incubation of 1 h at 37 C induces leakage in the GUV allowing the buffer containing FAM to penetrate inside the GUV. This experiment signifies that AB36_siRNA complex can cause poration and escape early endosome to cytoplasm. Escape from early endosome is an important criterion as in late endosome the pH turns more acidic which can be detrimental for maintaining the functionality of the siRNA.

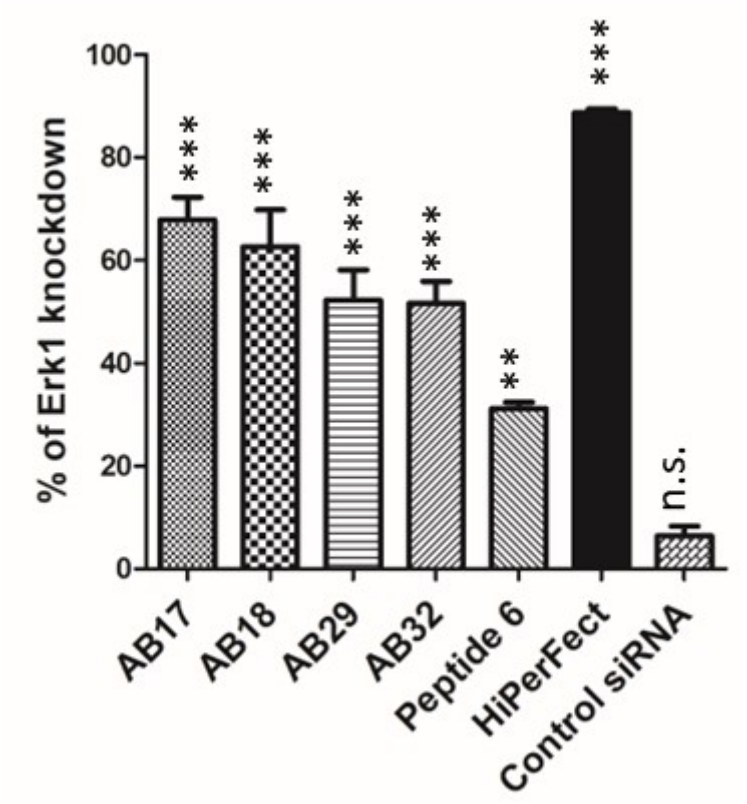

Figure S23. Real-Time PCR analysis of percentage of Erk1 gene knockdown at mRNA level in MDA-MB-231 cells by lipopeptide_ERK1/2 silencing siRNA complex after 48 h incubation at molar ratio 50 (lipopeptide:siRNA). At 48 h time point, HiPerFect_ERK1/2 silencing siRNA complex exhibited the highest level of knockdown efficiency (***$p<0.0001$, **$p<0.01$ and n.s.- not significant compared to untreated cells).

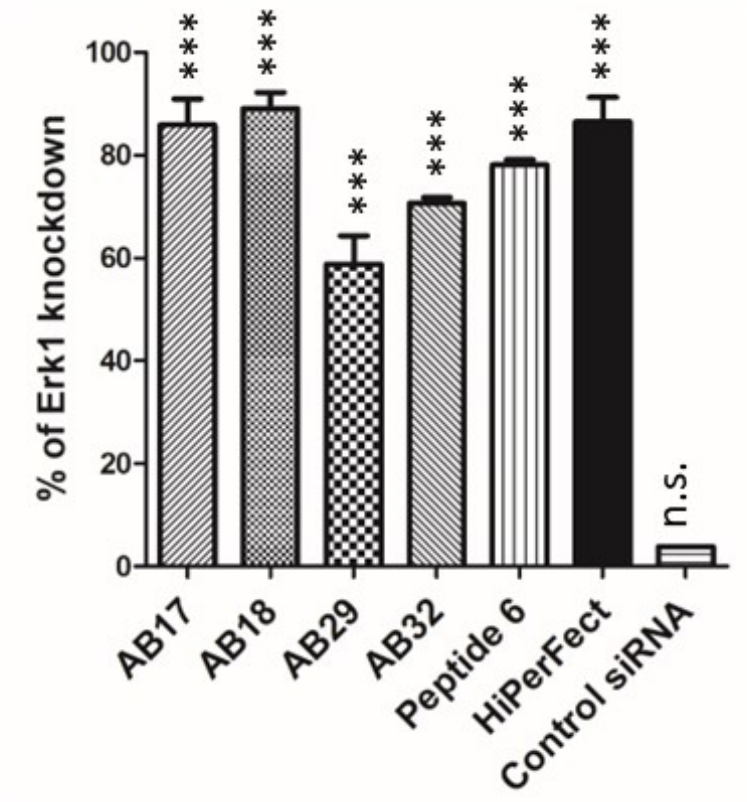

Figure S24. Real-Time PCR analysis of percentage of Erk1 gene knockdown at mRNA level in MDA-MB-231 cells by lipopeptide_ERK1/2 silencing siRNA complex after 72 h of incubation at molar ratio 50 (lipopeptide:siRNA). Result shows the lipopeptide_ERK1/2 silencing siRNA complexes show high level of knockdown of Erk1 gene (***$p<0.0001$ and n.s.- not significant compared to untreated cells).

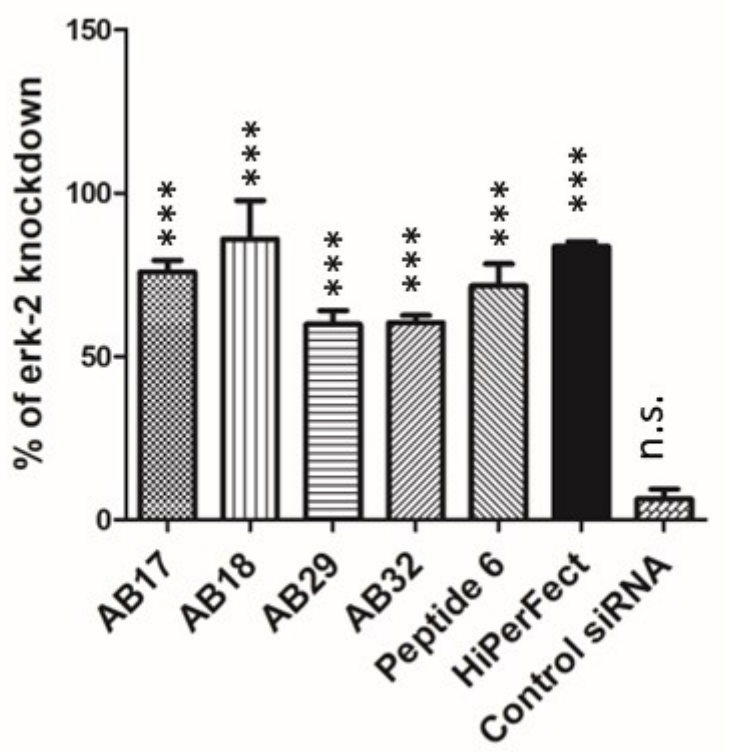

Figure S25. Real-Time PCR analysis of percentage of Erk2 gene knockdown at mRNA level in MDA-MB-231 cells by lipopeptide_ERK1/2 silencing siRNA complex after 72 h of incubation at molar ratio 50 (lipopeptide:siRNA). Result shows the lipopeptide_ERK1/2 silencing siRNA complexes show high level of knockdown of Erk2 gene (***$p<0.0001$ and n.s.- not significant compared to untreated cells).

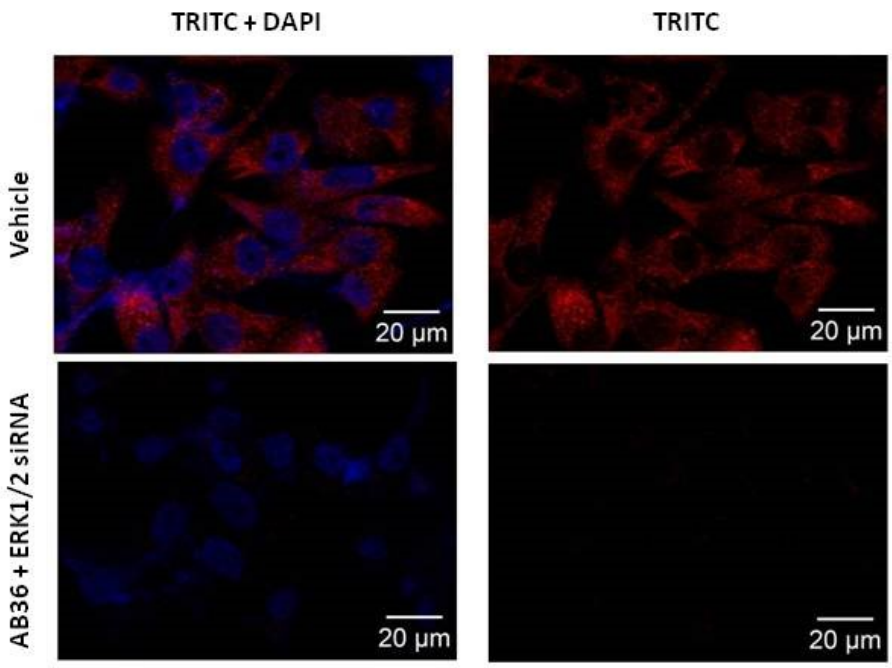

Figure S26. Immunofluorescence of ERK1/2 protein in MDA-MB-231 cells after transfection with unlabelled lipopeptide AB36_ERK1/2 silencing siRNA complex (MR=50) after 72 h of incubation. Red colour represents ERK1/2 protein expression and blue represents DAPI. ERK1/2 protein expression is highly lowered in MDA-MB-231 cells after transfection with AB36_ERK1/2 silencing siRNA complex compared to vehicle.

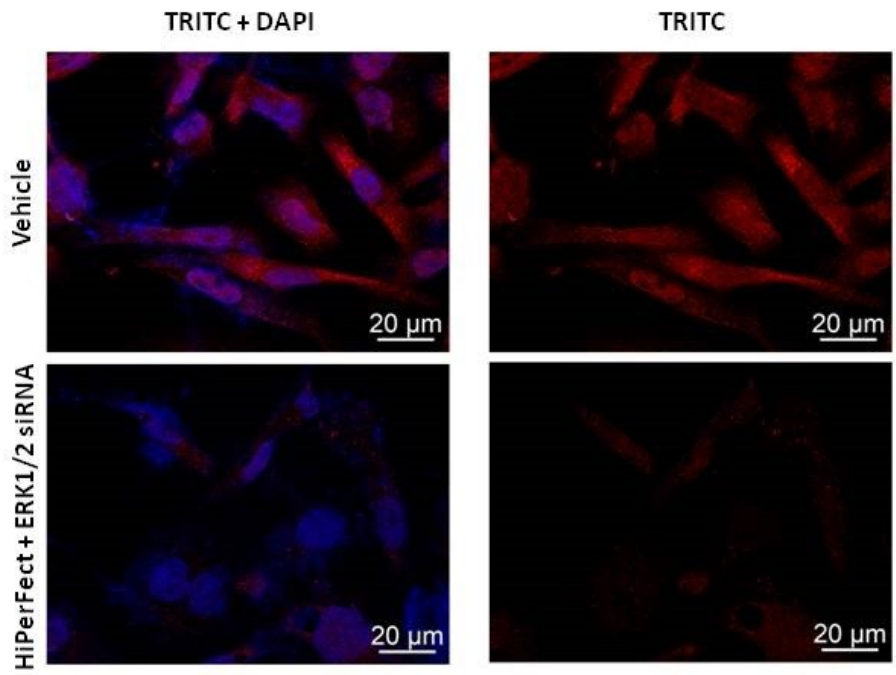

Figure S27. Immunofluorescence of ERK1/2 protein in MDA-MB-231 cells after transfection with HiPerFect_ERK1/2 silencing siRNA complex after 72 h of incubation. Red colour represents ERK1/2 protein expression and blue represents DAPI. ERK1/2 protein expression is lowered less by HiPerFect_ERK1/2 silencing siRNA complex in comparison to transfection with AB36_ERK1/2 silencing siRNA complex (Figure S23.)

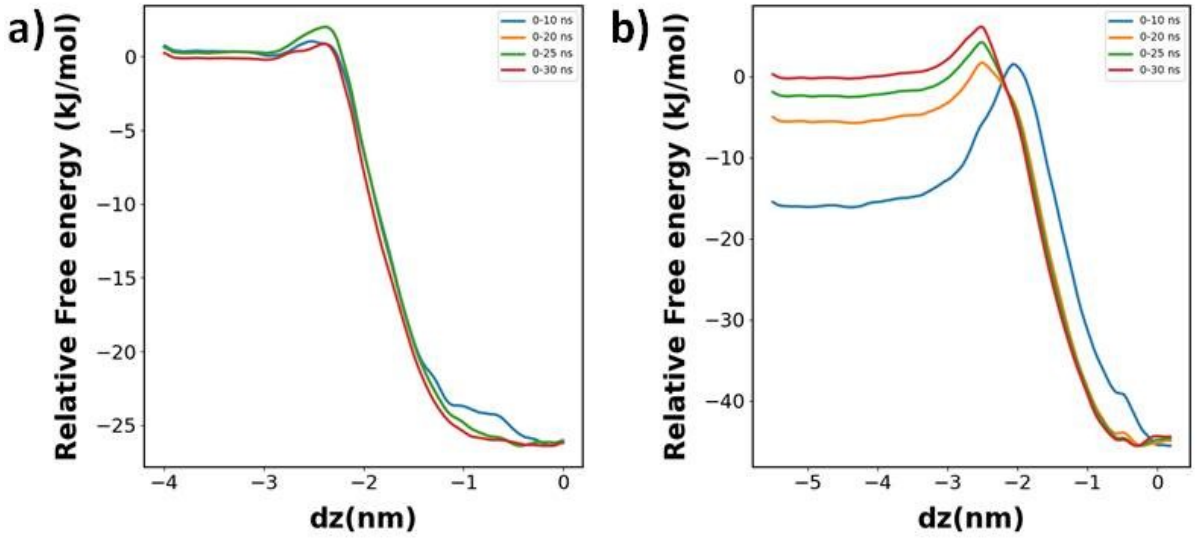

Figure S28. Convergence of free energy surface a) ADM b) Sub-vitE. These plots show that free energy surfaces are not changing with time and are thus converged.